Received 25 July 2022, accepted 11 August 2022, date of publication 29 August 2022, date of current version 12 September 2022.
Digital Object Identifier 10.1109/ACCESS.2022.3202933

RESEARCH ARTICLE

Improving the Response of an Electrohydrostatic Actuation (EHA) System Using a High-Pressure Accumulator

HYUNG-TAE SEO[1], (Member, IEEE), YUN-PYO HONG[2], (Member, IEEE), JIHYUK PARK[3], (Member, IEEE), AND KYUNG-SOO KIM[4], (Member, IEEE)
[1]Samsung Advanced Institute of Technology, Yeongtong-gu, Suwon-si, Gyeonggi-do 16678, Republic of Korea
[2]Advanced Packaging Group, Manufacturing Technology Center, Samsung Electronics, Hwaseong-si, Kyunggi-do 18448, Republic of Korea
[3]Department of Automotive Engineering, College of Mechanical and IT Engineering, Yeungnam University, Gyeongsan, Gyeongbuk 38541, Republic of Korea
[4]Department of Mechanical Engineering, Korea Advanced Institute of Science and Technology, Yuseong-gu, Daejeon 34141, Republic of Korea

Corresponding authors: Jihyuk Park (jihpark@yu.ac.kr) and Kyung-Soo Kim (kyungsookim@kaist.ac.kr)

This work was supported by the Project titled Development of Smart Port Autonomous Ships Linkage Technology funded by the Ministry of Oceans and Fisheries, South Korea.

ABSTRACT In this paper, we propose a novel hydraulic actuation system driven in three modes to improve the response of the existing electrohydrostatic actuation (EHA) system. By using a high-pressure accumulator, a servo valve, and mode switching valves, the hydraulic circuit can be switched to suit each mode according to the operational conditions. Each of the three modes consists of the EHA mode, the hybrid mode, and the charge mode, and the EHA mode operates on the same principle as the existing EHA system. Particularly, the hybrid mode is activated when high-speed position control is required, and with the help of an add-on servo valve controller, the control volume of the hydraulic cylinder can be stiffened quickly while minimizing the use of highly pressurized fluid. The charge mode serves to periodically charge the accumulator under motionless conditions in applications that allow piston holding. Through simulations and experiments, it was confirmed that the response of the proposed system is much improved compared to that of the existing EHA system.

INDEX TERMS Electrohydrostatic actuation, high-pressure accumulator, hybrid actuation, add-on control, mode switching.

I. INTRODUCTION

Still, the hydraulic actuation system has an unrivaled high power density compared to other actuation systems. For this reason, hydraulic systems have been applied to many robots and heavy machinery [1], [2]. In particular, electrohydraulic (EH) systems, which use a hydraulic reservoir and servo valve, are highly responsive and highly applicable. However, applying EH systems in mobile systems is difficult due to their heavy and bulky hydraulic components [3], [4]. To address the limitations, the development of an electrohydrostatic actuation (EHA) system for general industry began competitively in the late 1990s, along with miniaturization, weight reduction, and improvement of the controllability of the hydraulic components and electric motors [5], [6], [7]. The EHA system, also known as the variable-speed pump-controlled hydraulic servo system, does not require a large reservoir and has the advantage of high efficiency [8]. Nevertheless, this system has some systematic limitations. 1) the dynamic response is limited due to the high rotational inertia of its servomotor and bidirectional pump [9]; 2) pump nonlinearities, including dead zones and friction, can degrade the system performance; and 3) even pilot-operated check valves (POCVs), which represent compensation of the volume difference between control volumes in a passive way, may slow system actuation due to pressure-based operating conditions [10].

The research of EHA system has focused on achieving higher energy efficiency by modifying it to have a structure for energy storage and energy regeneration [11], [12],

The associate editor coordinating the review of this manuscript and approving it for publication was Tao Wang.

[13], [14], [15]. Nevertheless, systematic limitations of EHA apparently still exist: 1) the dynamic response is limited due to the high rotational inertia of its servomotor and bidirectional pump [9]; 2) pump nonlinearities, including dead zones and friction, can degrade the system performance; and 3) even pilot-operated check valves (POCVs), which passively compensate for the difference in the control volumes, may slow the actuation of the system due to pressure-based operating conditions [10]. To address the response limitations, [16] and [17] replaced the POCVs with limited throttling compensating valves to improve the performance of the EHA system over the entire operating range. The performance is largely dependent on the pump and motor. A novel EHA structure associated with a power regulator has been proposed in [18]. Although high power levels can be obtained instantaneously, the proportional valve has difficulty in guaranteeing a high control bandwidth.

In this paper, we newly propose a response-improved EHA system with a secondary flow source. To supply an additional pressurized flow, the secondary circuit consists of a high-pressure accumulator and a servo valve. Because the proposed system has three operation modes according to the configurations of the mode-switching valves, the operational principles of each mode is analyzed, and a multi-input single-output (MISO) nonlinear dynamic model of the proposed system is derived. To achieve a higher response while minimizing the discharge flow rate from the high-pressure accumulator, a reference-based proportional-differential (PD) servo-valve controller is added to the existing pump controller. Simulation studies and experimental evaluations verify that the response in the hybrid actuation mode is greatly improved compared to that of the conventional EHA system. Furthermore, by selecting an appropriate accumulator and using the charge mode, the proposed system can be used in applications that allow periodic position holding.

This paper is organized as follows: In Section II, the novel hybrid hydraulic actuation system with a high response is proposed and analyzed. In Section III, the design of the add-on servo-valve controller is presented. In Section IV, the control method is verified through both simulations and experiments. The conclusions are presented in Section V.

II. NOVEL HYBRID ACTUATION SYSTEM WITH A HIGH-PRESSURE ACCUMULATOR

A. PROPOSED SYSTEM CONFIGURATION AND OPERATION MODES

The new concept of the hybrid actuation system with a highly pressurized flow source is shown in Fig. 1. The pressure-generating structure is divided into a primary control part, a safety part, a reservoir part, mode-switching valves and a secondary control part. The secondary control part, similar to the secondary controlled drive concept [19], [20], is composed of a high-pressure accumulator that is appropriately selected according to the application and a servo

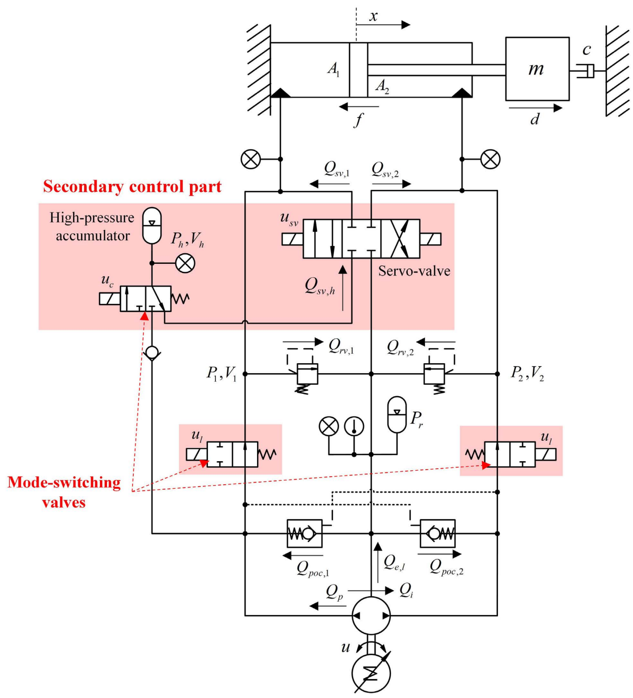

FIGURE 1. Diagram of the proposed hydraulic actuation system with a high-pressure accumulator.

valve. To minimize the energy loss in a compact structure, an additional passive capacitive element (*i.e.*, a high-pressure accumulator), instead of a large pump and a motor, is chosen. Then, the servo valve supplies the exact amount of pressurized flow in the accumulator. Additionally, the mode-switching valves are solenoid valves used for cylinder holding and accumulator charging. The low-pressure accumulator is used as a reservoir and absorbs the surge pressure. Note that the primary control, safety valve, and reservoir are the same as those used in the conventional EHA circuit.

The following three modes can be selected by suitably controlling the bidirectional pump, servo valve and mode-switching valves.

1) ELECTROHYDROSTATIC ACTUATION (EHA) MODE

In the EHA mode in Fig. 2(a), the 2-way/2-position mode-switching valves are opened, and the servo valve is in a neutral position. This mode has almost the same performance as the conventional EHA system in which the discharged flow from the pump produces a pressure change of the two control volumes. This mode is therefore used in situations in which maximizing the efficiency at a low response is desired.

2) HYBRID ACTUATION MODE

In the hybrid actuation mode in Fig. 2(b), the 2-way/2-position mode-switching valves are opened, and the orifice of the servo valve is continuously controlled. In this mode, the highly pressurized flow of the accumulator is supplied to the required control volume through the orifice of the servo valve, as shown in Fig. 3. Therefore, this mode is used in

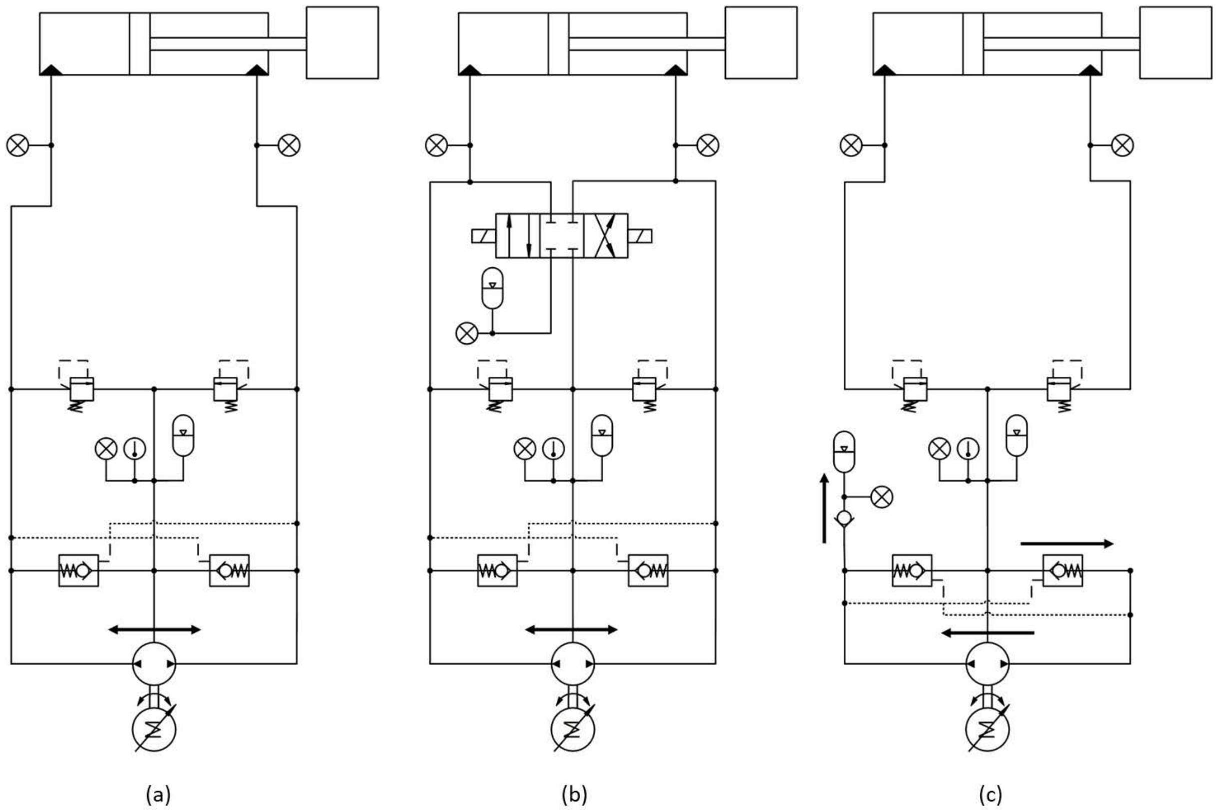

FIGURE 2. Operation modes of the proposed system: (a) EHA mode; (b) hybrid actuation mode; (c) charge mode.

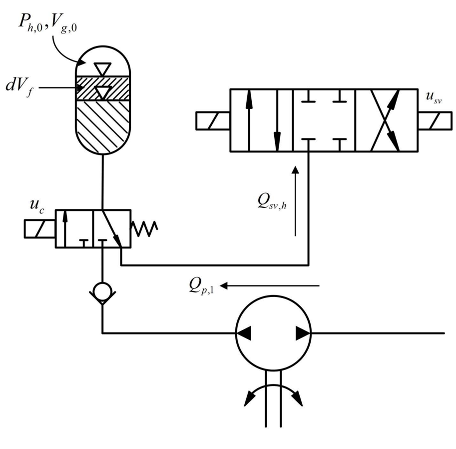

FIGURE 3. Schematic diagram of a secondary control part.

situations that require instantaneous rapid movement, such as high-frequency reference tracking. Because the performance of the hybrid actuation mode is expected to be highly dependent on the performance of the servo valve and charged pressure of the high-pressure accumulator, a further analysis is provided in Section C.

3) CHARGE MODE (WITH PISTON HOLDING)

The charge mode in Fig. 2(c) is required when additional flow cannot be supplied during the hybrid actuation mode or the accumulator pressure drops. In this mode, the 2-way/2-position mode-switching valves are closed, and the 3-way/2-position solenoid valve is fully opened, allowing the discharged flow from the pump to accumulate in the accumulator. At this time, the cylinder pistons are held against the internal pressure. Although the charging process may degrade the energy efficiency, we can address this inefficiency by properly selecting the application and effectively using piston holding through high-level control.

B. DYNAMIC MODEL OF THE PROPOSED SYSTEM

Basic thermal-hydraulic components can be separated into two categories, resistive components and capacitive components [21].

1) RESISTIVE COMPONENTS

In the proposed system in Fig. 1, the pump, relief valves, POCVs, and accumulators are resistive components.

First, the discharged flow rates $Q_{p,1}$ and $Q_{p,2}$ through the bidirectional hydraulic pump can be described as

$$\begin{aligned} Q_{p,1} &= D_p\dot{\theta}_p - k_i\left(P_1 - P_2\right) - k_{e,1}\left(P_1 - P_r\right) \\ Q_{p,2} &= -D_p\dot{\theta}_p + k_i\left(P_1 - P_2\right) - k_{e,2}\left(P_2 - P_r\right), \end{aligned} \tag{1}$$

where $\dot{\theta}_p$ is the angular velocity of the pump, D_p is the pump displacement, P_1 and P_2 are the pressures at each port, P_r is the reference pressure, k_i is the internal leakage coefficient, and $k_{e,1}$ and $k_{e,2}$ are external leakage coefficients.

Additionally, the flow rate $Q_{poc,1}$ through the POCV, which solves the physically nonsensical problem when using a differential cylinder, in the forward direction is derived as

$$Q_{poc} = C_{poc,D}A_{poc}\sqrt{\frac{2}{\rho}}\frac{\tilde{P}_{poc}}{\left(\tilde{P}_{poc}^2 + P_{poc,cr}^2\right)^{1/4}}, \tag{2}$$

where $C_{poc,D}$ is the flow discharge coefficient, $P_{poc,cr}$ is the critical pressure, and $\tilde{P}_{poc} = P_A - P_B$. Here, the effective pressure $\bar{P}_{poc} = P_A + k_{poc,p}P_X - P_B$ given by the force balance in the POCV structure can be defined to calculate the orifice area A_{poc}. The orifice area A_{poc} is determined by the pressure-based condition as follows:

$$A_{poc} = \begin{cases} A_{poc,l} & \bar{P}_{poc} < P_{poc,cr} \\ A_{poc,l} + k_{poc}\left(\bar{P}_{poc} - P_{poc,cr}\right) & P_{poc,cr} \le \bar{P}_{poc} < P_{poc,\max} \\ A_{poc,\max} & \bar{P}_{poc} \ge P_{poc,\max} \end{cases} \tag{3}$$

where k_{poc} is the orifice area coefficient, $P_{poc,cr}$ and $P_{poc,\max}$ are the cracking pressure for valve opening and the maximum pressure for the maximally opened state, respectively, and $A_{poc,l}$ and $A_{poc,\max}$ are the orifice areas in the closed state and maximally opened state, respectively.

Additionally, from Fig. 3, the flow rate Q_a through each accumulator is simply given as

$$Q_a = \frac{dV_f}{dt}, \tag{4}$$

V_f is the fluid volume in the accumulator, which can be modeled mathematically by

$$\begin{aligned} P_{h,0}V_{g,0}^k &= P_h\left(V_{g,0} - \int_0^t Q_a dt\right)^k \quad \text{adiabatic condition} \\ P_{h,0}V_{g,0} &= P_h\left(V_{g,0} - \int_0^t Q_a dt\right) \quad \text{isothermal condition} \end{aligned} \tag{5}$$

where P_h is the current pressure of the accumulator, $P_{h,0}$ is the initial pressure of the accumulator, $V_{g,0}$ is the initial volume of the gas chamber, and k is the polytropic exponent of gas, which ranges from 1.0 to 1.4.

2) CAPACITIVE COMPONENTS

The capacitive component can be assumed to have a fluid volume inside it. In this sense, the proposed system in Fig. 1 has three capacitive components. For each capacitive component, the basic equations for hydraulic modeling from the flow continuity equation for one-dimensional flow are given by

$$\frac{dP}{dt} = \beta\left[\frac{1}{V}\left(\sum Q_{in} - \sum Q_{out} - \frac{dV}{dt}\right)\right], \tag{6}$$

where β is the bulk modulus.

Finally, the dynamic equations for Fig. 1 are obtained as follows by adding the equations for the flow in and out of the servo valve provided in the high-pressure accumulator.

$$\begin{aligned} m\ddot{x} + c\dot{x} &= (A_1P_1 - A_2P_2) - f + d \\ \dot{P}_1 &= \frac{\beta}{V_{1,0} + A_1x} \times \left[Q_{p,1} + Q_{poc,1} - Q_{rv,1} + Q_{sv,1} - A_1\dot{x}\right] \\ \dot{P}_2 &= \frac{\beta}{V_{2,0} - A_2x} \times \left[Q_{p,2} + Q_{poc,2} - Q_{rv,2} + Q_{sv,2} + A_2\dot{x}\right] \\ \dot{P}_h &= \frac{\beta}{V_h} \times \left[Q_{p,1}sgn(u_c) - Q_{sv,h}\left\{1 - sgn(u_c)\right\} - Q_a\right] \end{aligned} \tag{7}$$

where $u_c \ge 0$ is the input of the 3-way/2-position solenoid valve and

$$\begin{aligned} Q_{sv,1} &= \begin{cases} \gamma_1 x_v\sqrt{P_h - P_1} & x_v \ge 0 \\ \gamma_1 x_v\sqrt{P_1 - P_r} & x_v < 0 \end{cases} \\ Q_{sv,2} &= \begin{cases} \gamma_2 x_v\sqrt{P_2 - P_r} & x_v \ge 0 \\ \gamma_2 x_v\sqrt{P_h - P_2} & x_v < 0 \end{cases} \\ Q_{sv,h} &= \begin{cases} \gamma_1 x_v\sqrt{P_h - P_1} & x_v \ge 0 \\ \gamma_2 x_v\sqrt{P_h - P_2} & x_v < 0 \end{cases} \end{aligned} \tag{8}$$

C. ANALYSIS OF SECONDARY CONTROL PART

The secondary control part in Fig. 3 discharges additional fluid in the hybrid actuation mode and charges the fluid from the reservoir in the charge mode. Here, because the high-pressure accumulator is used for energy storage, the pressure of the accumulator, P_h, should always be higher than the maximum operating pressure. For this purpose, the charging time should be as short as possible, and the discharge time should be as long as possible.

First, in the charge mode ($u_c > 0$), the accumulator can be rapidly charged from the pump. Weand regard this process as an adiabatic process as in the first equation of (5).

However, in the hybrid actuation mode ($u_c = 0$), the secondary control part can be regarded as an isothermal state when it supplies a relatively small amount of pressurized fluid in one accumulator cycle. Therefore, under the assumption that $Q_{sv,h}$ is constant, the current pressure of the accumulator is explicitly obtained by combining the second equation of (5) and the last equation of (7) and using $P_h(0) = P_{h,0}$ as follows.

$$P_h = \left[\frac{P_{h,0}}{2} - \frac{\beta}{2V_h}V_{g,0} - \frac{\beta}{2V_h}Q_{sv,h}t\right] + \sqrt{\left[\frac{P_{h,0}}{2} - \frac{\beta}{2V_h}V_{g,0} - \frac{\beta}{2V_h}Q_{sv,h}t\right]^2 + \frac{\beta}{V_h}P_{h,0}V_{g,0}}, \tag{9}$$

Then, given that the ratio between $P_{h,0}$ and the maximum operating pressure is noted with the factor ε, where

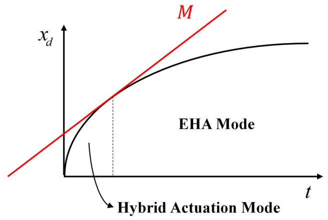

FIGURE 4. Mode switching method according to the slope of the reference.

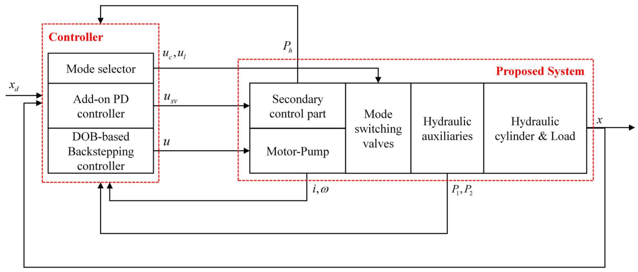

FIGURE 5. Overall control configuration.

$0 < \varepsilon < 1$, the discharging time of the accumulator from $P_{h,0}$ to $\varepsilon P_{h,0}$ is derived as

$$t = \frac{1-\varepsilon}{\varepsilon} \frac{\varepsilon P_{h,0} V_h + \beta V_{g,0}}{\beta Q_{sv,h}}. \tag{10}$$

Based on the above equation, to use the accumulator once it has charged for a sufficient period of time, the volume of the secondary control part should be increased, and the flow rate discharged from the accumulator, $Q_{sv,h}$, should be minimized. To achieve this, we propose an add-on position controller design method that gives a higher response while minimizing the discharge flow rate in the following section.

III. ADD-ON CONTROL STRATEGY

The hybrid actuation circuit and hydraulic actuator proposed in Fig. 1 operate with the pump flow controlled by the motor and the flow rate of the accumulator controlled by the servo valve. Thus, the system with two degrees of freedom has one purpose of controlling the position of the piston of the hydraulic cylinder using a dual control strategy with two inputs. That is, when a high response is needed, the flow input of (8) controlled by the servo valve is applied, and when the pump motor is controlled, (1) is considered.

A. BIDIRECTIONAL PUMP CONTROLLER

The EHA mode involves inherent nonlinear functions, system uncertainties, and mismatched disturbances. To address these limitations, we combine a disturbance observer and a backstepping pump controller based on the identified nonlinear model in (7).

B. SERVO-VALVE CONTROLLER

To achieve the long-term use of the accumulator flow and to minimize heat generation, we adopt an add-on-type hybrid control concept that provides only the additional flow required for the flow supplied by the pump.

Because the servo valve operates only in the hybrid actuation mode, we design a PD controller that is activated under conditions of rapid change in the reference position. Specifically, when the slope of the reference position value of the piston is below the predetermined value M, the system operates in the EHA mode, and it switches to the hybrid actuation mode when the slope is larger than the predetermined value. The switching function is defined as follows:

$$f(\dot{x}_d) = \begin{cases} |\dot{x}_d| & |\dot{x}_d| \geq M \\ 0 & |\dot{x}_d| < M. \end{cases} \tag{11}$$

The switching function is shown in Fig. 4. The final add-on control input can be expressed as

$$u_a = f(\dot{x}_d)\left(k_p (x_d - x) + k_d (\dot{x}_d - \dot{x})\right), \tag{12}$$

where k_p and k_d are control gains.

Consequently, the overall control block diagram is shown in Fig. 5. The mode selector determines the position of the mode switching valves to enter the charge mode when maintaining the current position.

IV. SIMULATION STUDIES

The simulation is performed in the AMESim/MATLAB environment as shown in Fig. 6. A controller block designed in the MATLAB/simulink environment is applied to the model constructed in the AMESim, a leading commercial simulation software in the field of hydraulic systems. The performance parameters of the pump and servo valve are set at a maximum pressure of 140 bar and a maximum flow of 6 lpm, and the maximum stroke of the hydraulic cylinder piston is set at 0.072 m. Additionally, nonlinearities such as friction, dead zones, and hydraulic resistance are considered. Here, the

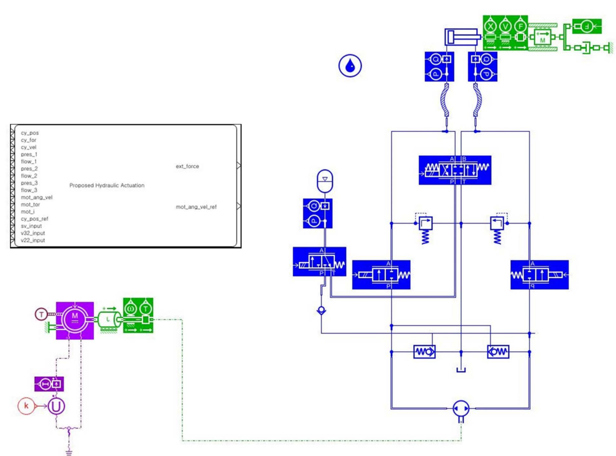

FIGURE 6. Hydraulic simulator for the proposed system in the AMESim environment.

process in the N_2 gas chamber of the accumulator is assumed to be polytropic. In particular, the polytropic index is set to 1.55. To verify the performance of the proposed approach, the following three cases are given.

- *Case 1*: The position reference is a step signal, , *i.e.,* , $x_d = 0.02 \cdot u_s(t-2) - 0.02 \cdot u_s(t-3)[m]$.
- *Case 2*: The position reference is a chirp signal from 0.3 Hz to 6 Hz.
- *Case 3*: The position reference is a periodic position reference with holding.

A. CASE 1: STEP POSITION REFERENCE

The step reference tracking results are shown in Fig. 7. In the hybrid actuation mode, the rise time is improved by approximately 60% compared to the conventional EHA circuit. As shown in Fig. 8, a step reference instantaneously causes a large flow rate from the servo valve. However, we can see that the pump uses less flow, which means that hybrid control works.

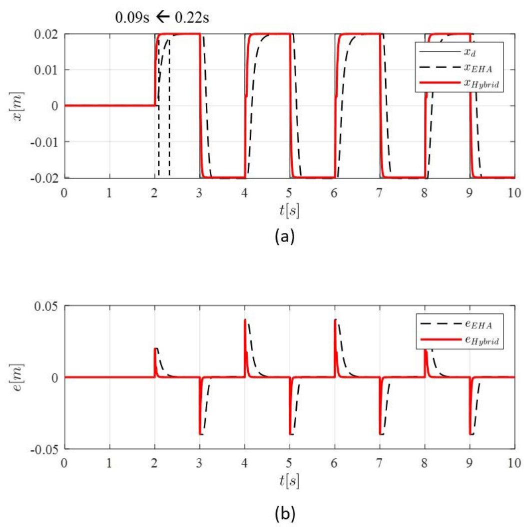

FIGURE 7. Step reference tracking performance for each actuation (Hybrid: proposed actuation) in simulation.((a)Tracking position and (b)error).

B. CASE 2: CHIRP POSITION REFERENCE

In the simulation, the pump of the proposed system has the ability to follow a position reference signal of approximately 0.5 Hz. Therefore, in the reference tracking within 0.7 Hz, only the EHA mode is operated. Therefore, in Fig. 9 and Fig. 10, the operation of the proposed actuation system is similar to that of the conventional EHA system.

However, based on the reference tracking above 0.7 Hz, the proposed system has a much higher control bandwidth due to the hybrid actuation mode.

C. CASE 3: PERIODIC POSITION REFERENCE WITH HOLDING

To test the feasibility of the overall operation, including the charge mode, a reference position signal with a high

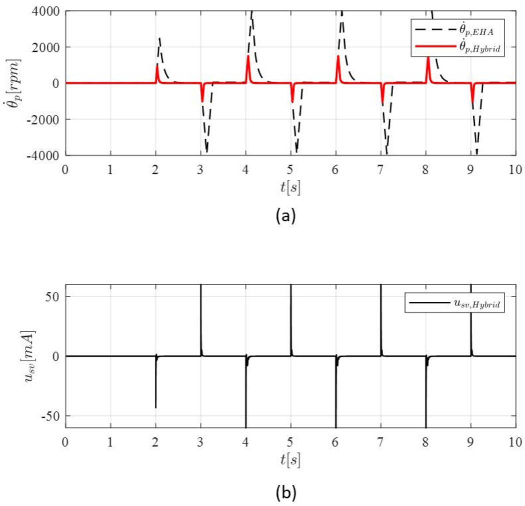

FIGURE 8. (a)Pump angular velocity and (b)servo-valve input for each actuation in step reference tracking in simulation.

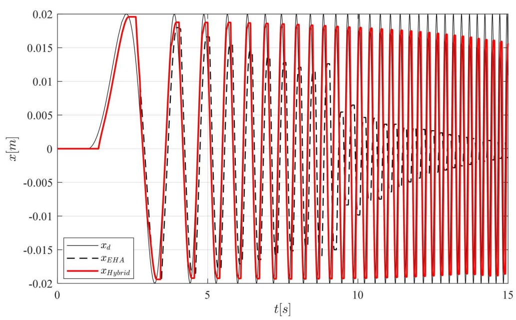

FIGURE 9. Chirp reference tracking performance for each actuation (Hybrid: proposed actuation) in simulation.

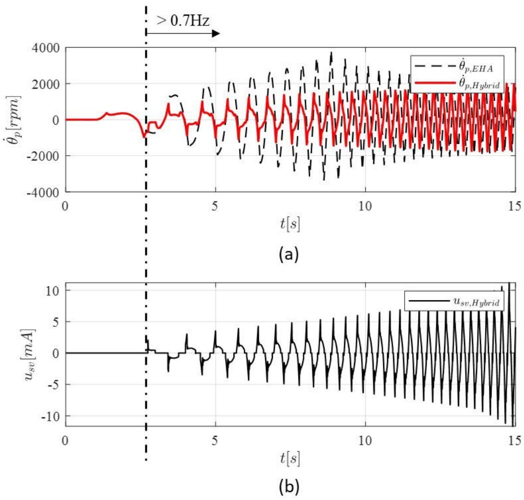

FIGURE 10. (a)Pump angular velocity and (b)servo-valve input for each actuation in chirp reference tracking in simulation.

frequency region, a low frequency region, and a holding region is arbitrarily generated. The proposed system has a faster rise time and a higher bandwidth than the conventional

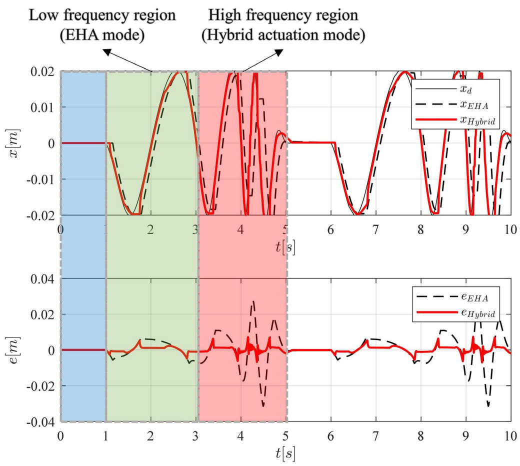

FIGURE 11. **Periodic reference tracking performance for each actuation (Hybrid: proposed actuation) in simulation.((a)Tracking position and (b)error).**

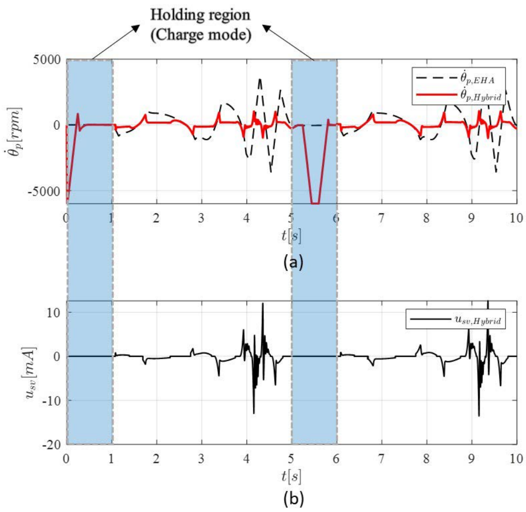

FIGURE 12. **(a)Pump angular velocity and (b)servo-valve input for each actuation in periodic reference tracking in simulation.**

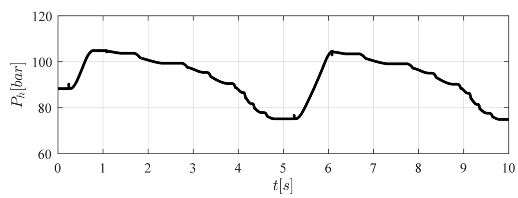

FIGURE 13. **Pressure of the high-pressure accumulator in periodic reference tracking in simulation.**

EHA system, as shown in Fig. 11. Additionally, Fig. 12 shows that the EHA mode is set for the low-frequency reference signal, the hybrid actuation mode is set for the high-frequency reference signal, and the charge mode is set for holding, so mode switching occurs in the entire operation region. Remarkably, the pressure of the fluid in the accumulator is maintained above a certain level, as shown in Fig. 13.

V. EXPERIMENTAL EVALUATIONS

A. EXPERIMENTAL ENVIRONMENT

The test bench includes four manifolds with a hydraulic power pack, a secondary control part, and a reservoir. Additionally, pressure sensors are integrated to measure the pressure in the cylinder chamber outside the manifold, and a linear variable differential transformer (LVDT) is connected to the end of the piston so that the position of the cylinder can be measured. In particular, the electrohydraulic two-stage servo valve is used. Note that the volume of the accumulator selected in the experiment is large compared to the volume of fluid discharged during one cycle. However, the accumulator does not need to be large because it is controlled to minimize the accumulator usage by the add-on controller concept discussed in Section III. Therefore, although the current test bench is a low-cost version, if all components are replaced with miniature components and the integrated manifold design is used, the addition of four valves and one accumulator may not significantly change the overall weight and volume, and a compact design is still possible with the proper manifold design. The specifications shown in Fig. 14 are listed in Table 1.

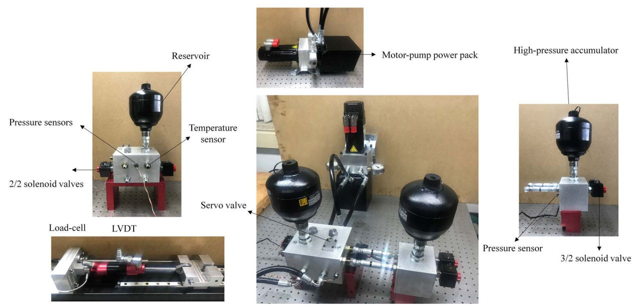

FIGURE 14. **Test bench of the proposed system.**

To ensure the real-time operation of the control system, the experiments are conducted in a *Real-time Windows Target* environment of MATLAB with a $1kHz$ sampling rate.

The experiment is conducted to verify the performance of the proposed hydraulic actuation, and the following two references are given.

- *Case 1*: The position reference is a step signal, , *i.e.,* , $x_d = 0.01 \cdot u_s(t) - 0.01 \cdot u_s(t - 1.5)[m]$.
- *Case 2*: The position reference is a $0.8Hz$ sine signal, , *i.e.,* , $x_d = 0.01 \cdot \sin(2\pi \cdot 0.8t)[m]$.

B. CASE 1: STEP POSITION REFERENCE

The reference tracking simulation results are shown in Fig. 15. Due to the hybrid actuation mode, the rise time is improved by approximately 28% compared to that of the conventional EHA system.

C. CASE 2: SINE POSITION REFERENCE

For reference signal tracking above 0.5 Hz, the system periodically switches between the EHA mode and the hybrid

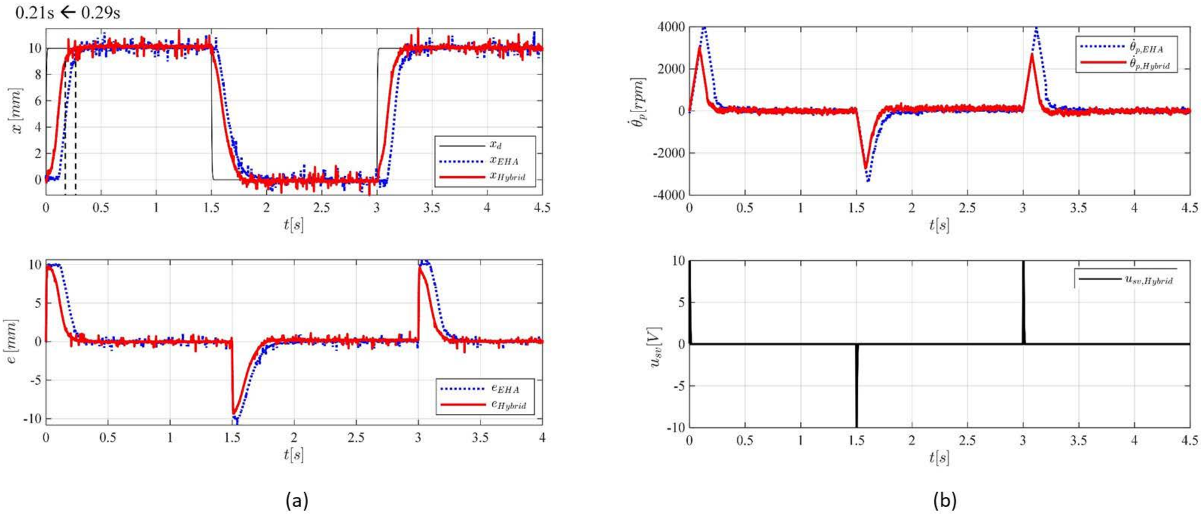

FIGURE 15. Simulation results for the step position reference, (a) reference tracking performance of secondary control, (b) control inputs of controllers ($x_d = 0.01 \cdot u_s(t) - 0.01 \cdot u_s(t - 1.5)[m]$).

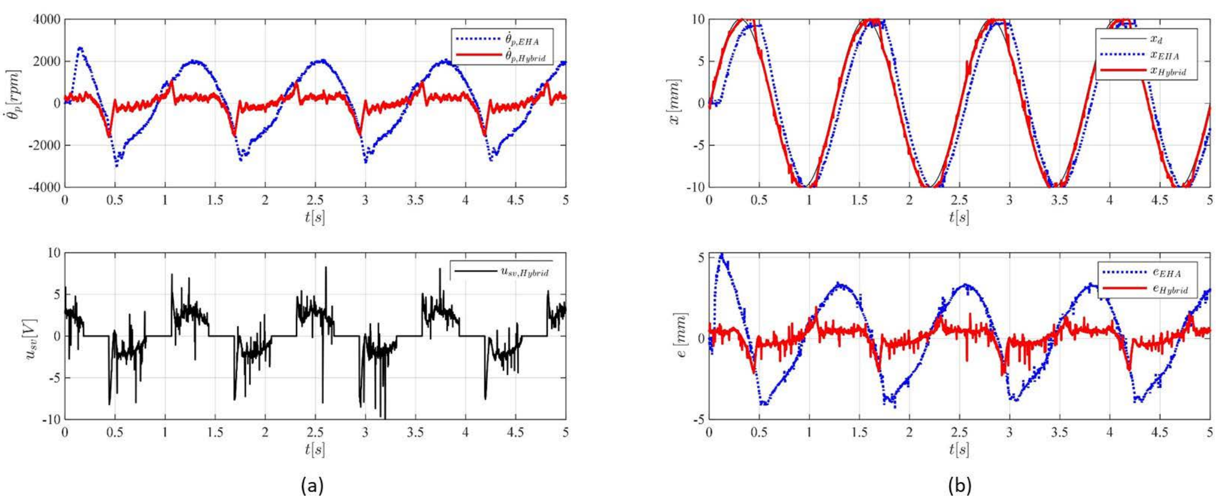

FIGURE 16. Simulation results for the sine position reference, (a) servo-valve input and accumulator pressure change, (b) reference tracking performance of secondary control ($x_d = 0.01 \cdot \sin(2\pi \cdot 0.8t)[m]$).

TABLE 1. Specifications of the test bench.

Parameters	Specifications
Max operating pressure	140 bar
Max operating flow rate	4 lpm
Cylinder stroke	72 mm
Cylinder diameter	20 mm
Piston rod diameter	10 mm
Pump displacement	1 cc/rev
Power ofBLDC motor	1.2 kW
Max speed of BLDC motor	6000 rpm
Nominal volume of high-pressure accumulator	0.16 l
Gas charging pressure of high-pressure accumulator	53.6 bar
Nominal volume of low-pressure accumulator	0.32 l

actuation mode, as shown in Fig. 16(a). This switching results in a higher frequency behavior and increases the tracking frequency and rise time. The results are shown in Fig. 16(b).

VI. CONCLUSION

In this paper, a novel hydraulic actuation system with a passive auxiliary circuit using a high-pressure accumulator has been proposed. Since there are three operation modes (EHA mode, hybrid actuation mode, and charge mode) according to the position of each directional valve, the operational principles of each mode was analyzed. In addition, to maximize the efficiency of the hybrid actuation mode, a reference-based PD add-on controller that provides an additional flow rate has been applied to achieve the required performance. Simulation studies and experimental evaluations verified that the proposed system is capable of providing a higher frequency behavior by rapidly stiffening the control volume. Furthermore, mode switching, including the charge mode, has been shown to continuously occur in the entire operation region for the system that performs periodic movement.

REFERENCES

[1] T. Yu, A. R. Plummer, P. Iravani, J. Bhatti, S. Zahedi, and D. Moser, ''The design, control, and testing of an integrated electrohydrostatic powered ankle prosthesis,'' *IEEE/ASME Trans. Mechatronics*, vol. 24, no. 3, pp. 1011–1022, Jun. 2019.

[2] L. Huang, T. Yu, Z. Jiao, and Y. Li, ''Research on power matching and energy optimal control of active load-sensitive electro-hydrostatic actuator,'' *IEEE Access*, vol. 9, pp. 51121–51133, 2020.

[3] Z. Quan, L. Quan, and J. Zhang, ''Review of energy efficient direct pump controlled cylinder electro-hydraulic technology,'' *Renew. Sustain. Energy Rev.*, vol. 35, pp. 336–346, Jul. 2014.

[4] S. Ketelsen, D. Padovani, T. Andersen, M. Ebbesen, and L. Schmidt, ''Classification and review of pump-controlled differential cylinder drives,'' *Energies*, vol. 12, no. 7, p. 1293, Apr. 2019.

[5] S. Habibi and A. Goldenberg, ''Design of a new high performance electrohydraulic actuator,'' in *Proc. IEEE/ASME Int. Conf. Adv. Intell. Mechatronics*, Sep. 1999, pp. 227–232.

[6] Z. Jiao, Z. Li, Y. Shang, S. Wu, Z. Song, and Q. Pan, ''Active load sensitive electro-hydrostatic actuator on more electric aircraft: Concept, design, and control,'' *IEEE Trans. Ind. Electron.*, vol. 69, no. 5, pp. 5030–5040, May 2022.

[7] E. Jalayeri, A. Imam, Z. Tomas, and N. Sepehri, ''A throttle-less single-rod hydraulic cylinder positioning system: Design and experimental evaluation,'' *Adv. Mech. Eng.*, vol. 7, no. 5, pp. 1–4, 2015.

[8] A. Helbig, ''Electro-hydrostatic actuation: An Attractive energy-efficient option for machine builders,'' Moog Inc., New York, NY, USA, White Paper CDL44033-en, 2014. [Online]. Available: https://www.moog.com/content/dam/moog/literature/ICD/Moog-Actuators-EHA-Whitepaper-en.pdf

[9] N. Alle, S. S. Hiremath, S. Makaram, K. Subramaniam, and A. Talukdar, ''Review on electro hydrostatic actuator for flight control,'' *Int. J. Fluid Power*, vol. 17, no. 2, pp. 125–145, May 2016.

[10] A. Imam, M. Rafiq, E. Jalayeri, and N. Sepehri, ''Design, implementation and evaluation of a pump-controlled circuit for single rod actuators,'' *Actuators*, vol. 6, no. 1, p. 10, Feb. 2017.

[11] K. K. Ahn, T. H. Ho, and Q. T. Dinh, ''A study on energy saving potential of hydraulic control system using switching type closed loop constant pressure system,'' in *Proc. JFPS Int. Symp. Fluid Power*, vol. 7, no. 2, 2008, pp. 317–322.

[12] T. H. Ho and K. K. Ahn, ''Modeling and simulation of hydrostatic transmission system with energy regeneration using hydraulic accumulator,'' *J. Mech. Sci. Technol.*, vol. 24, no. 5, pp. 1163–1175, May 2010.

[13] Y. Shang, X. Li, H. Qian, S. Wu, Q. Pan, L. Huang, and Z. Jiao, ''A novel electro hydrostatic actuator system with energy recovery module for more electric aircraft,'' *IEEE Trans. Ind. Electron.*, vol. 67, no. 4, pp. 2991–2999, Apr. 2020.

[14] Q. Zhou, S. Guo, L. Xu, X. Guo, H. Williams, H. Xu, and F. Yan, ''Global optimization of the hydraulic-electromagnetic energy-harvesting shock absorber for road vehicles with human-knowledge-integrated particle swarm optimization scheme,'' *IEEE/ASME Trans. Mechatronics*, vol. 26, no. 3, pp. 1225–1235, Jun. 2021.

[15] M. Wang, Y. Wang, Y. Fu, R. Yang, J. Zhao, and J. Fu, ''Experimental investigation of an electro-hydrostatic actuator based on the novel active compensation method,'' *IEEE Access*, vol. 8, pp. 170635–170649, 2020.

[16] A. Imam, M. Rafiq, E. Jalayeri, and N. Sepehri, ''A pump-controlled circuit for single-rod cylinders that incorporates limited throttling compensating valves,'' *Actuators*, vol. 7, no. 2, p. 13, Mar. 2018.

[17] A. Imam, M. Rafiq, T. Zeljko, and N. Sepehri, ''Improving the performance of pump-controlled circuits for single-rod actuators,'' *Actuators*, vol. 8, no. 1, p. 26, Mar. 2019.

[18] K. Rongjie, J. Zongxia, W. Shaoping, and C. Lisha, ''Design and simulation of electro-hydrostatic actuator with a built-in power regulator,'' *Chin. J. Aeronaut.*, vol. 22, no. 6, pp. 700–706, Dec. 2009.

[19] R. Kordak, *Hydrostatic Transmission Drives With Secondary Control*. Lohr a. Main, Germany: Bosch Rexroth, 2003.

[20] X. Guo, X. Ji, J. Hu, Z. Peng, and C. Jing, ''Numerical simulation and dynamic characteristics of secondary controlled hydrostatic drive,'' in *Proc. Int. Conf. Mechatronics Autom.*, Aug. 2007, pp. 2099–2103.

[21] L. Chenggong and J. Zongxia, ''Calculation method for thermal-hydraulic system simulation,'' *J. Heat Transf.*, vol. 130, no. 8, p. 084503, Aug. 2008.

[22] W. Lee, M. J. Kim, and W. K. Chung, ''Asymptotically stable disturbance observer-based compliance control of electrohydrostatic actuators,'' *IEEE/ASME Trans. Mechatronics*, vol. 25, no. 1, pp. 195–206, Feb. 2020.

[23] D. Won, W. Kim, D. Shin, and C. C. Chung, ''High-gain disturbance observer-based backstepping control with output tracking error constraint for electro-hydraulic systems,'' *IEEE Trans. Control Syst. Technol.*, vol. 23, no. 2, pp. 787–795, Mar. 2015.

HYUNG-TAE SEO (Member, IEEE) received the B.S., M.S., and Ph.D. degrees in mechanical engineering from the Department of Mechanical Engineering, Korea Advanced Institute of Science and Technology (KAIST), Daejeon, South Korea, in 2011, 2013, and 2020, respectively. He is currently with the Samsung Advanced Institute of Technology (SAIT), Suwon, South Korea, as a Staff Researcher. His research interests include mobile robots, control of hydraulic actuation systems, and robust control theories, including disturbance observer-based control.

YUN-PYO HONG (Member, IEEE) received the M.S. and Ph.D. degrees in mechanical engineering from the Department of Mechanical Engineering, Korea Advanced Institute of Science and Technology (KAIST), Daejeon, South Korea, in 2014 and 2021, respectively. He is currently with the Samsung Mechatronics Research and Development Center, Hwaseong-si, Gyeonggi-do, as a Staff Engineer. His research interests include pneumatic actuators and their power source generation module, including the design of a pneumatically actuated mobile robot and its high-performance mechatronic system design.

JIHYUK PARK (Member, IEEE) received the B.S. and Ph.D. degrees in mechanical engineering from the Korea Advanced Institute of Science and Technology, Daejeon, South Korea, in 2011 and 2018, respectively. He was a Staff Engineer at the Mechatronics Research and Development Center, Samsung Electronics Company. He is currently an Assistant Professor at the Department of Automotive Engineering, Yeungnam University. His research interests include mechatronic systems, control of robotic systems, vibration control, autonomous driving, machine learning in robotics, and indoor/outdoor navigation.

KYUNG-SOO KIM (Member, IEEE) received the B.S., M.S., and Ph.D. degrees in mechanical engineering from KAIST, Daejeon, South Korea, in 1993, 1995, and 1999, respectively. He was a Chief Researcher with LG Electronics Inc., from 1999 to 2003, and a DVD Front-End Manager with STMicroelectronics Company Ltd., from 2003 to 2005. In 2005, he joined the Department of Mechanical Engineering, Korea Polytechnic University, Gyeonggi, South Korea, as a Faculty Member. Since 2007, he has been with the Department of Mechanical Engineering, KAIST, and serves as an Associate Editor for *Automatica* and the *Journal of Mechanical Science and Technology*. His research interests include control theory, sensor and actuator design, and robot manipulator design.